Available online at www.sciencedirect.com
ScienceDirect
Surface Science 601 (2007) 450–459
SURFACE SCIENCE
www.elsevier.com/locate/susc

Surface currents on a perfect conductor, induced by a magnetic dipole

Henk F. Arnoldus *

Department of Physics and Astronomy, Mississippi State University, P.O. Drawer 5167, Mississippi State, MS 39762-5167, USA

Received 21 March 2006; accepted for publication 3 May 2006
Available online 30 October 2006

Abstract

An oscillating magnetic dipole located near a perfect conductor induces a current density on the surface of the metal. We have derived an expression for this current density, and studied its field line patterns for various orientations of the dipole moment. When the dipole moment is perpendicular to the surface, the field lines are circles which run clockwise and counterclockwise. For a linear dipole oriented parallel to the surface, the field line pattern is much more complex, and it contains singular points. When the dipole moment rotates in a plane parallel to the surface, the field lines are spirals. A field line spirals inward from infinity to some given point, after which it spirals outward back to infinity. We have also considered the Poynting vector of the electromagnetic field near the surface, and we found that its field lines can have singular points or exhibit a vortex.

Keywords: Light scattering; Metallic surfaces; Metal-insulator interfaces

1. Introduction

Singularities in an electromagnetic radiation field may occur as phase discontinuities in traveling waves [1], but the most intriguing singular phenomenon in radiation is the optical vortex. In such a vortex the field lines of the Poynting vector, indicating the direction of energy flow, swirl around a line. For a point on this line the direction of the Poynting vector is usually undetermined, which makes the line a singular line. The first prediction of the appearance of a vortex seems to have been made by Braunbek and Laukien [2], who showed that when a half-infinite screen is illuminated by a plane wave a vortex line appears. This line runs parallel to the screen, and is located near the edge at the illuminated side. Such a vortex is the result of diffraction, and similar vortices appear for instance in diffraction through a narrow slit [3,4]. A particular interesting example is the occurrence of vortices in Laguerre–Gaussian laser beams [5–8], where the appearance of the vortices reflects the angular momentum carried by the beam [9,10].

Vortices of a different nature occur when the rotation in the field lines of the Poynting vector has its origin in the source emitting the radiation, rather than being a result of diffraction or interference. When a small source, like an atom, emits a pure electric or magnetic multipole field of order (ℓ, m), with $m \neq 0$, the radiation exhibits a vortex [11], and the appearance of the vortex is a reflection of the angular momentum carried by the light [12]. Fig. 1 shows two field lines for a dipole ($\ell = 1$) with $m = 1$. The extend of the vortex is less than a wavelength. The field lines spiral around the z-axis near the origin, and at larger distances they run approximately radially outward. We shall consider the situation where an oscillating magnetic dipole is located near the surface of a perfectly conducting metal. Such a magnetic dipole can be realized, for instance, by crossing an atomic beam with a laser beam near the surface. The laser frequency is tuned to an electric-dipole-forbidden, but magnetic-dipole-allowed atomic transition, and the laser polarization is chosen such as to excite a particular mode of oscillation of the dipole (for instance, circular around the normal to the surface). The resonance fluorescence emitted by an atom of the beam is then magnetic dipole radiation as considered here, provided that line

* Tel.: +1 662 325 2919; fax: +1 662 325 8898.
E-mail address: arnoldus@ra.msstate.edu

0039-6028/$ - see front matter © 2006 Elsevier B.V. All rights reserved.
doi:10.1016/j.susc.2006.05.063

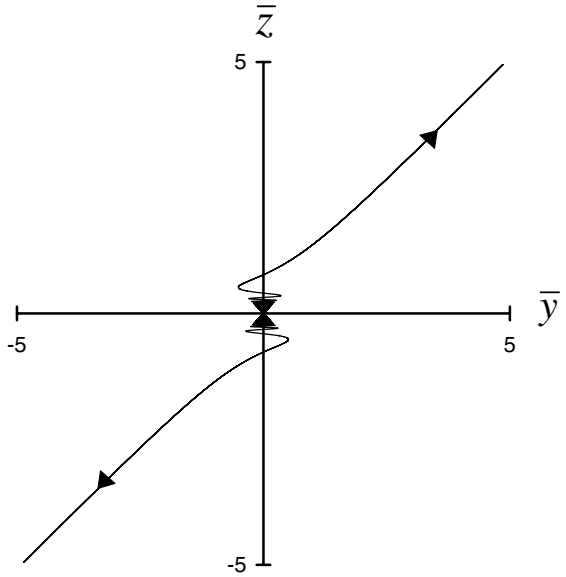

Fig. 1. Shown in this figure are two field lines of the Poynting vector of the radiation field emitted by a dipole with $m = 1$, located at the origin of coordinates. For $m = 1$ dipole radiation, the light carries angular momentum, and the energy flow exhibits the vortex structure shown. We use dimensionless coordinates $\bar{x} = k_0 x$, etc., with k_0 the wave number. Then $\Delta\bar{x} = 2\pi$ corresponds to one wavelength. We see from the figure that the extend of the vortex around the origin is well below a wavelength.

broadening due to spontaneous emission is ignored. The radiation field of such a dipole will induce a surface current in the material, and it can be anticipated that the current density has an intricate field line pattern, in particular when the radiation field itself contains a vortex as in Fig. 1. The corresponding case for an electric dipole was considered in Ref. [12], where it was shown that for $m = 1$ the field lines of the current density in the xy-plane lie inside an infinite spiral. It turns out that for a magnetic dipole the result is far more complex.

2. Field of a magnetic dipole near a perfect conductor

A magnetic dipole has a dipole moment $\boldsymbol{p}(t)$, and we shall assume a harmonic time dependence

$$\boldsymbol{p}(t) = \mathrm{Re}(\boldsymbol{p}\mathrm{e}^{-\mathrm{i}\omega t}), \tag{1}$$

with $\boldsymbol{p}$ a constant, in general complex-valued, vector and ω the angular frequency. The emitted electric field $\boldsymbol{E}(\boldsymbol{r}, t)$ then has the same time dependence, e.g.,

$$\boldsymbol{E}(\boldsymbol{r}, t) = \mathrm{Re}[\boldsymbol{E}(\boldsymbol{r})\mathrm{e}^{-\mathrm{i}\omega t}], \tag{2}$$

with $\boldsymbol{E}(\boldsymbol{r})$ the complex amplitude, and similarly the magnetic field $\boldsymbol{B}(\boldsymbol{r}, t)$ has complex amplitude $\boldsymbol{B}(\boldsymbol{r})$. For a magnetic dipole located at the origin of coordinates these fields are [13]

$$\boldsymbol{E}(\boldsymbol{r}) = \frac{k_0^3}{4\pi\varepsilon_0 c}\boldsymbol{p}\times\hat{\boldsymbol{r}}\left(1+\frac{i}{q}\right)\frac{\mathrm{e}^{\mathrm{i}q}}{q}, \tag{3}$$

$$\boldsymbol{B}(\boldsymbol{r}) = \frac{\mu_0 k_0^3}{4\pi}\left\{\boldsymbol{p}-(\boldsymbol{p}\cdot\hat{\boldsymbol{r}})\hat{\boldsymbol{r}}+[\boldsymbol{p}-3(\boldsymbol{p}\cdot\hat{\boldsymbol{r}})\hat{\boldsymbol{r}}]\frac{i}{q}\left(1+\frac{i}{q}\right)\right\}\frac{\mathrm{e}^{\mathrm{i}q}}{q}, \tag{4}$$

with $k_0 = \omega/c$ the wave number, $\hat{\boldsymbol{r}}$ the radial unit vector, and $q = k_0 r$ the dimensionless radial distance between the field point $\boldsymbol{r}$ and the dipole.

The surface of the perfect conductor will be taken as the xy-plane, and we consider the dipole located on the z-axis, a distance H above the surface. The total field in the region $z > 0$ is then the emitted field given by Eqs. (3) and (4), shifted up over a distance H, and the field of the image dipole $\boldsymbol{p}^{\mathrm{im}}$. The image dipole is positioned on the z-axis, a distance H below the surface. If we write $\boldsymbol{p} = \boldsymbol{p}_{\parallel} + \boldsymbol{p}_{\perp}$ for the dipole moment, with the subscripts referring to the orientation with respect to the surface, then the image dipole moment is given by [14] $\boldsymbol{p}^{\mathrm{im}} = \boldsymbol{p}_{\parallel} - \boldsymbol{p}_{\perp}$. Its field is again given by Eqs. (3) and (4), with $\boldsymbol{p}$ replaced by $\boldsymbol{p}^{\mathrm{im}}$, and shifted down over a distance H.

3. Surface current density

The fields of the magnetic dipole and its mirror image induce a surface current density $\boldsymbol{i}(\boldsymbol{r}, t)$ in the xy-plane. The complex amplitude $\boldsymbol{i}(\boldsymbol{r})$ follows in the usual way from a boundary condition for the magnetic field:

$$\boldsymbol{i}(\boldsymbol{r}) = \frac{1}{\mu_0}\boldsymbol{e}_z \times \boldsymbol{B}(\boldsymbol{r}), \tag{5}$$

with $\boldsymbol{B}(\boldsymbol{r})$ the magnetic field just above the xy-plane. In order to evaluate $\boldsymbol{B}(\boldsymbol{r})$ in the xy-plane we consider the setup shown in Fig. 2. The field point $\boldsymbol{r}$ is in the xy-plane, and vectors $\boldsymbol{r}_1$ and $\boldsymbol{r}_2$ represent this point with respect to the dipole and the image dipole, respectively. The variable q in Eqs. (3) and (4) is the dimensionless distance between the source and the field point, which is now $q_1 = k_0 r_1$ for the dipole, and since the field point is in the xy-plane, this distance is the same for the image dipole. We shall use again

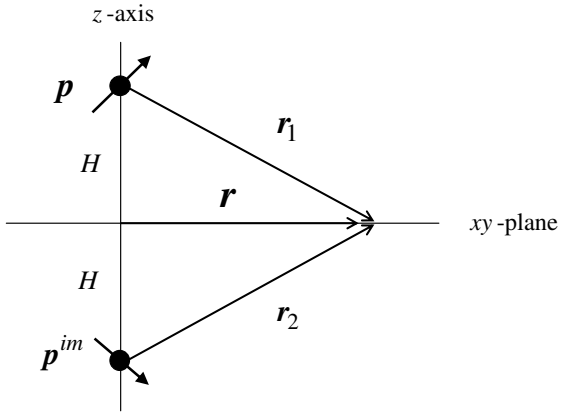

Fig. 2. The magnetic dipole $\boldsymbol{p}$ is located on the z-axis, a distance H above the xy-plane. Its mirror image $\boldsymbol{p}^{\mathrm{im}}$ is a distance H below the xy-plane, and it has its perpendicular component reversed, as compared to $\boldsymbol{p}$. A point in the xy-plane is represented by the position vector $\boldsymbol{r}$ with respect to the origin of coordinates, and by $\boldsymbol{r}_1$ and $\boldsymbol{r}_2$ with respect to the dipole and its mirror image, respectively.

$q = k_0 r$ for the distance between the field point and the origin of coordinates. When we set $h = k_0 H$ for the dimensionless distance between the dipole and the surface, we have

$$q_1 = \sqrt{q^2 + h^2}, \tag{6}$$

as follows from the figure. The unit vector $\hat{\boldsymbol{r}}$ in Eqs. (3) and (4) has to be replaced by $\hat{\boldsymbol{r}}_1$ for the dipole and by $\hat{\boldsymbol{r}}_2$ for the image dipole. We shall indicate by $\boldsymbol{e}_\rho$ the radial unit vector in the xy-plane, so that $\boldsymbol{r} = r\boldsymbol{e}_\rho$. It then follows from the figure that

$$\hat{\boldsymbol{r}}_1 = \frac{1}{q_1}(q\boldsymbol{e}_\rho - h\boldsymbol{e}_z), \tag{7}$$

$$\hat{\boldsymbol{r}}_2 = \frac{1}{q_1}(q\boldsymbol{e}_\rho + h\boldsymbol{e}_z). \tag{8}$$

Putting everything together then yields for the magnetic field in the xy-plane

$$\boldsymbol{B}(\boldsymbol{r}) = \frac{\mu_0 k_0^3}{2\pi}\left[\boldsymbol{p}_\parallel\left(1 + \frac{i}{q_1} - \frac{1}{q_1^2}\right) - \frac{q}{q_1^2}(q\boldsymbol{p}_\parallel \cdot \boldsymbol{e}_\rho - hp_\perp)\boldsymbol{e}_\rho\left(1 + \frac{3i}{q_1} - \frac{3}{q_1^2}\right)\right]\frac{\mathrm{e}^{\mathrm{i}q_1}}{q_1}, \tag{9}$$

with $p_\perp = \boldsymbol{p}\cdot\boldsymbol{e}_z$. We notice that $\boldsymbol{B}(\boldsymbol{r})$ is in the xy-plane, as is required by the boundary conditions for a perfect conductor.

The complex amplitude of the current density, $\boldsymbol{i}(\boldsymbol{r})$, then follows from Eq. (5), after which the time-dependent current density is

$$\boldsymbol{i}(\boldsymbol{r}, t) = \mathrm{Re}[\boldsymbol{i}(\boldsymbol{r})\mathrm{e}^{-\mathrm{i}\omega t}]. \tag{10}$$

The dipole moment can be written as

$$\boldsymbol{p} = p_0 \mathrm{e}^{\mathrm{i}\psi}\boldsymbol{\varepsilon}, \tag{11}$$

with $p_0 > 0$, ψ a real-valued phase factor, and $\boldsymbol{\varepsilon}$ a unit vector, which in general will be complex valued. Then we set

$$i_0 = \frac{k_0^3 p_0}{2\pi}, \tag{12}$$

and introduce the time parameter

$$\alpha = \omega t - \psi, \tag{13}$$

which then finally yields for the current density

$$\boldsymbol{i}(\boldsymbol{r}, t) = i_0 \mathrm{Re}\left\{\left[\boldsymbol{e}_z \times \boldsymbol{\varepsilon}_\parallel\left(1 + \frac{i}{q_1} - \frac{1}{q_1^2}\right) - \frac{q}{q_1^2}(q\boldsymbol{\varepsilon}_\parallel \cdot \boldsymbol{e}_\rho - h\varepsilon_\perp) \times \boldsymbol{e}_\phi\left(1 + \frac{3i}{q_1} - \frac{3}{q_1^2}\right)\right]\frac{\mathrm{e}^{\mathrm{i}(q_1 - \alpha)}}{q_1}\right\}, \tag{14}$$

with $\boldsymbol{e}_\phi = \boldsymbol{e}_z \times \boldsymbol{e}_\rho$.

4. Dipole moment along the z-axis

Let us first consider the case where the magnetic dipole moment $\boldsymbol{p}$ is real and oriented along the z-axis. Then we have $\boldsymbol{\varepsilon}_\parallel = 0$, $\varepsilon_\perp = 1$, and Eq. (14) simplifies to

$$\boldsymbol{i}(\boldsymbol{r}, t) = \frac{i_0 hq}{q_1^3}\boldsymbol{e}_\phi\left[\left(1 - \frac{3}{q_1^2}\right)\cos(q_1 - \alpha) - \frac{3}{q_1}\sin(q_1 - \alpha)\right]. \tag{15}$$

For a given time t, or a given α, the current density is in the $\boldsymbol{e}_\phi$ direction, and its magnitude only depends on q (and parametrically on h). The field lines of $\boldsymbol{i}(\boldsymbol{r}, t)$ are circles around the origin, as illustrated in Fig. 3. Since $\boldsymbol{i}(\boldsymbol{r}, t)$ is proportional to q, we have $\boldsymbol{i}(\boldsymbol{r}, t) = 0$ at the origin of coordinates. At $\boldsymbol{r} = 0$ the direction $\boldsymbol{i}(\boldsymbol{r}, t)$ is undetermined, and therefore $\boldsymbol{r} = 0$ is a singular point in the field line pattern. Furthermore, the factor in square brackets in Eq. (15) is zero when q is a solution of

$$\tan(q_1 - \alpha) = \frac{q_1}{3} - \frac{1}{q_1}. \tag{16}$$

Each solution q determines a circle in the xy-plane. If we cross such a circle, then the factor in square brackets in Eq. (15) changes sign, and so the current density reverses direction. We call these circles the singular circles, because on these circles the direction of $\boldsymbol{i}(\boldsymbol{r}, t)$ is undetermined.

Fig. 3 shows the field line pattern of $\boldsymbol{i}(\boldsymbol{r}, t)$ for a given instant t. When time progresses, the field line picture changes. Since the time dependence of $\boldsymbol{i}(\boldsymbol{r}, t)$ only enters as $\exp(-\mathrm{i}\omega t)$, any field line pattern repeats itself after a time $\Delta t = 2\pi/\omega$. If we consider a fixed point $\boldsymbol{r}$, then $\boldsymbol{i}(\boldsymbol{r}, t)$ oscillates back and forth with angular frequency ω, while remaining tangent to a circle at all times. In order to see how the pattern of Fig. 3 evolves in time, we consider the singular circles. The (dimensionless) radius q of such a circle is a solution of the transcendental Eq. (16), and depends on time through the parameter α. By differentiating Eq. (16) with respect to α we derive

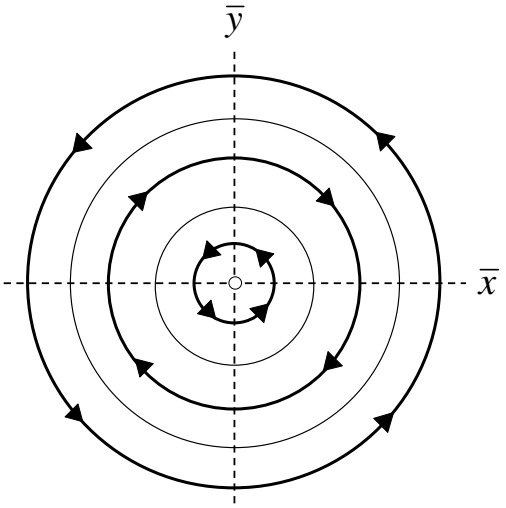

Fig. 3. Field line pattern of the current density $\boldsymbol{i}(\boldsymbol{r}, t)$ for a dipole moment along the z-axis. The thin lines are the singular circles on which the current density vanishes. Across such a circle $\boldsymbol{i}(\boldsymbol{r}, t)$ changes direction, so the current densities are counter rotating in two regions separated by a singular circle. The radii of all circles increase with time, and the circles are about half a wavelength apart.

$$\frac{\mathrm{d}q}{\mathrm{d}\alpha} = \sqrt{1+\frac{h^2}{q^2}} + \frac{3}{q_1 q}\left(1+\frac{3}{q_1^2}\right), \tag{17}$$

which is positive for any solution q. Therefore, the radii q of the singular circles increase with α, or t. This means that all circles in Fig. 3 expand with time, and new circles are continuously being produced at the origin. In terms of r and t we have

$$\frac{\mathrm{d}r}{\mathrm{d}t} = c\frac{\mathrm{d}q}{\mathrm{d}\alpha}, \tag{18}$$

which is the speed, or rate of expansion, of a singular circle. Since the right-hand side of Eq. (17) is larger than unity, we see that the rate of expansion of the singular circles is larger than the speed of light. For q large, the rate $\mathrm{d}r/\mathrm{d}t$ approaches the speed of light c.

5. Dipole moment parallel to the surface

As a second case we consider a real dipole moment, oriented parallel to the xy-plane, say along the x-axis. Then we have $\boldsymbol{\varepsilon}_{\parallel} = \boldsymbol{e}_x$, $\varepsilon_{\perp} = 0$, and the current density from Eq. (14) becomes

$$\boldsymbol{i}(\boldsymbol{r},t) = \frac{i_0}{q_1}\{\boldsymbol{e}_x b(q)\sin\phi\cos\phi + \boldsymbol{e}_y[a(q) - b(q)\cos^2\phi]\}. \tag{19}$$

Here we have introduced the abbreviations

$$a(q) = \left(1-\frac{1}{q_1^2}\right)\cos(q_1-\alpha) - \frac{1}{q_1}\sin(q_1-\alpha), \tag{20}$$

$$b(q) = \frac{q^2}{q_1^2}\left[\left(1-\frac{3}{q_1^2}\right)\cos(q_1-\alpha) - \frac{3}{q_1}\sin(q_1-\alpha)\right]. \tag{21}$$

These functions only depend on the coordinate q of the field point (not on ϕ), and they depend parametrically on h and α. In terms of the unit vectors $\boldsymbol{e}_\rho$ and $\boldsymbol{e}_\phi$ the current density is

$$\boldsymbol{i}(\boldsymbol{r},t) = \frac{i_0}{q_1}\{\boldsymbol{e}_\rho a(q)\sin\phi + \boldsymbol{e}_\phi[a(q) - b(q)]\cos\phi\}. \tag{22}$$

In order to analyze the field line pattern of the current density, we first determine the locations of the singularities, e.g., the points in the xy-plane where $\boldsymbol{i}(\boldsymbol{r},t)$ vanishes. For a point on the y-axis we have $\phi = \pm\pi/2$, and with Eq. (19) this gives

$$\boldsymbol{i}(\boldsymbol{r},t) = \frac{i_0}{q_1}a(q)\boldsymbol{e}_y \quad (y\text{-axis}), \tag{23}$$

with $q = y$. If we set $a(q) = 0$, then this is an equation for q, and each solution q can be considered to define a circle in the xy-plane. The points where these circles intersect the y-axis are the singular points on the y-axis. Fig. 4 shows $a(q)$ as a function of q for $h = 1$ and $\alpha = 0$. In general, the origin of coordinates, $q = 0$, will not be a singular point. For q large we have $a(q) \approx \cos(q-\alpha)$, and therefore the roots of $a(q)$ are approximately 2π apart. On the y-axis, $\boldsymbol{i}(\boldsymbol{r},t)$ is

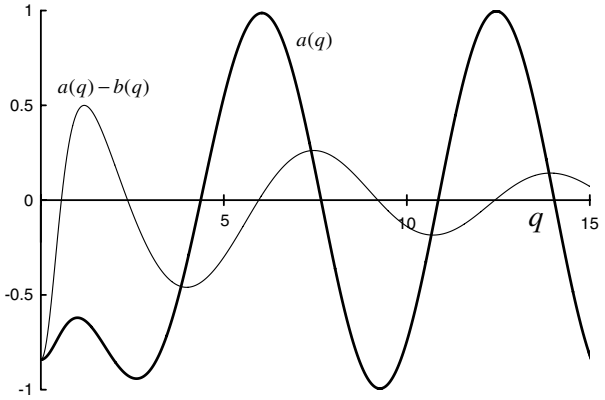

Fig. 4. The figure shows the graphs of the functions $a(q)$ (thick line) and $a(q) - b(q)$ (thin line) for $h = 1$ and $\alpha = 0$. The zeros of $a(q)$ determine the singular points on the y-axis, and from the data we obtain the solutions $q = 4.37, 7.66, 10.86, 14.03, \ldots$ The roots of $a(q) - b(q)$ give the singular points on the x-axis, and we find $q = 0.56, 2.37, 5.59, 9.21, 12.41, \ldots$

in the y-direction. When moving along the y-axis, the current density changes direction when we pass a singular point, since $a(q)$ changes sign. For a point on the x-axis we have $\phi = 0$ or π, and with Eq. (19) this gives

$$\boldsymbol{i}(\boldsymbol{r},t) = \frac{i_0}{q_1}[a(q) - b(q)]\boldsymbol{e}_y \quad (x\text{-axis}). \tag{24}$$

So, on the x-axis the current density is also in the y-direction, except at the singular points where $a(q) - b(q) = 0$. Fig. 4 shows $a(q) - b(q)$ as a function of q, and the roots of this function represent circles in the xy-plane. The points where these circles intersect the x-axis are the singular points on the x-axis. When moving along the x-axis, $\boldsymbol{i}(\boldsymbol{r},t)$ changes direction when we cross a singular point. For q large we have $a(q) - b(q) \approx (2/q)\sin(q-\alpha)$, as can be shown from Eqs. (20) and (21), and the roots are approximately 2π apart. Let us now consider a point (q,ϕ) off the coordinate axes. For $\boldsymbol{i}(\boldsymbol{r},t)$ to be zero, it follows from Eq. (22) that $a(q) = 0$ and $b(q) = 0$ have to hold simultaneously. It is easy to verify from Eqs. (20) and (21) that this is impossible. Therefore, all singular points are located on the coordinate axes.

On the y-axis, the current density is given by Eq. (23), and we see that $\boldsymbol{i}(\boldsymbol{r},t)$ is along the y-axis. Therefore the y-axis is a field line, except for the singular points across which the current density changes direction. The direction of the field line is determined by the sign of $a(q)$. For a point on a circle defined by $a(q) = 0$ we have from Eq. (22)

$$\boldsymbol{i}(\boldsymbol{r},t) = -\frac{i_0}{q_1}\boldsymbol{e}_\phi b(q)\cos\phi \quad (a = 0), \tag{25}$$

which is tangent to the circle. Therefore, these circles are field lines, except for the singular points on the y-axis. It follows from Eq. (22) that across such a circle the $\boldsymbol{e}_\rho$ component of $\boldsymbol{i}(\boldsymbol{r},t)$ changes sign, so the current density changes from flowing inward to flowing outward, or vice versa. The

direction of the current density on the circle follows from Eq. (25). On a circle $a(q) - b(q) = 0$ we have

$$\boldsymbol{i}(\boldsymbol{r},t) = \frac{i_0}{q_1}\boldsymbol{e}_\rho a(q)\sin\phi, \quad (a-b=0), \tag{26}$$

for which the current density is in the radial direction. Therefore, these circles are not field lines. We see from Eq. (22) that across such a circle the $\boldsymbol{e}_\phi$ component of $\boldsymbol{i}(\boldsymbol{r},t)$ changes sign. The direction of $\boldsymbol{i}(\boldsymbol{r},t)$ for a point on the x-axis is determined by the sign of $a(q) - b(q)$, according to Eq. (24), and $\boldsymbol{i}(\boldsymbol{r},t)$ changes direction across a circle $a(q) - b(q) = 0$. Fig. 5 illustrates the considerations so far.

Through every point, except a singular point, goes a field line, indicating the direction of the current flow at that point. This implies in particular that field lines can not cross. Let us now consider the point marked with ● in Fig. 5. This point is surrounded by two semi-circular field lines and by two field line segments on the $\bar{y}$-axis. Therefore, if we would follow the field line through ●, there is no way out of this area. In order to find out the remaining part of the field line picture, we resort to numerical integration. Let a field line be parametrized as $\boldsymbol{r} = \boldsymbol{r}(u)$, with u a dummy variable. Then at $\boldsymbol{r}$ on the curve, the current density $\boldsymbol{i}(\boldsymbol{r},t)$ is on the tangent line, and points into the direction of increasing u. Therefore, the field lines are solutions of the differential equation

$$\frac{\mathrm{d}\boldsymbol{r}}{\mathrm{d}u} = f(\boldsymbol{r})\boldsymbol{i}(\boldsymbol{r},t), \tag{27}$$

with $f(\boldsymbol{r})$ an arbitrary positive function of $\boldsymbol{r}$. We shall use the representation of Eq. (19) for $\boldsymbol{i}(\boldsymbol{r},t)$, and use dimensionless coordinates $\bar{x} = k_0 x$, $\bar{y} = k_0 y$. We take $f(\boldsymbol{r}) = q_1/(k_0 i_0)$, and substitute $\cos\phi = \bar{x}/q$, $\sin\phi = \bar{y}/q$, which then gives the set of equations

$$\frac{\mathrm{d}\bar{x}}{\mathrm{d}u} = b(q)\frac{\bar{x}\bar{y}}{q^2}, \tag{28}$$

$$\frac{\mathrm{d}\bar{y}}{\mathrm{d}u} = a(q) - b(q)\frac{\bar{x}^2}{q^2}, \tag{29}$$

with $q = (\bar{x}^2 + \bar{y}^2)^{\frac{1}{2}}$. For given initial values $(\bar{x}_0, \bar{y}_0)$, corresponding to for instance the coordinates of the point ● in Fig. 5, this set determines the coordinates $(\bar{x}, \bar{y})$ of the points on the field line through $(\bar{x}_0, \bar{y}_0)$ as a function of u. When the initial point is taken as in Fig. 5, we have to integrate forward and backward in u in order to obtain the entire field line.

The field line pattern for $\boldsymbol{i}(\boldsymbol{r},t)$ for the case of a dipole oscillating along the x-axis is shown in Fig. 6. We notice from Eq. (19) that $\boldsymbol{i}(\boldsymbol{r},t)$ is symmetric for reflection in the $\bar{y}$-axis (for $\phi \to \pi - \phi$ the i_x changes sign and the i_y remains unaltered), so we only show the result for $\bar{x} > 0$. It appears that most field lines start at a singular point on the $\bar{y}$-axis. They follow a circle $a(q) = 0$ for a while, and then turn either left or right. After that they catch up with an adjacent $a(q) = 0$ circle, and then they end at another singular point on the $\bar{y}$-axis. The only exception to this behavior is seen near the origin where some field lines form closed loops, rather than running from one singular point to another. These closed loops circle around the singular point on the $\bar{x}$-axis, given by the smallest solution of $a(q) - b(q) = 0$, e.g., the first zero of the thin curve in Fig. 4. A singular point on the $\bar{y}$-axis resembles a source or a sink in the sense that all field lines come out of this point or end up in this point (this is more clear in Fig. 5). We notice from Fig. 6 that the singular points on the $\bar{x}$-axis are of a different nature. For a given point, field lines flow to it and away from it, and in such a way that they appear to be repelled by the singular point.

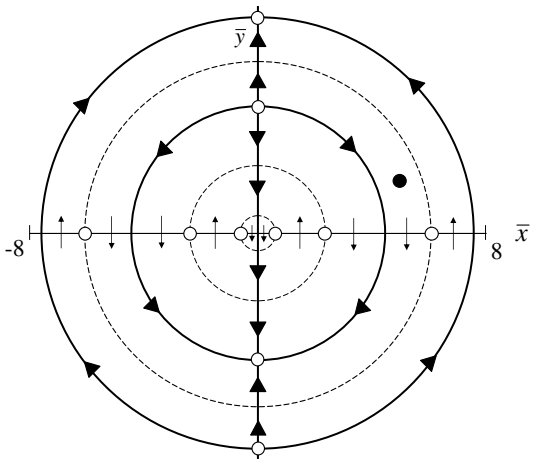

Fig. 5. The thick circles have a radius equal to the solution of $a(q) = 0$, and for this figure we have taken the numerical data from Fig. 4. Their intersections with the $\bar{y}$-axis are singular points of the flow field, and these are indicated by small circles. The dashed circles have a radius equal to the solution of $a(q) - b(q) = 0$, and their intersections with the $\bar{x}$-axis are singular points. The thick circles and the $\bar{y}$-axis are field lines, interrupted by singular points. The arrow heads indicate the directions of the various parts of the field lines. The arrows on the $\bar{x}$-axis indicate the direction of $\boldsymbol{i}(\boldsymbol{r},t)$ in that neighborhood. This direction reverses when crossing a dashed circle.

6. Rotating dipole moment

A different type of field line pattern appears when we take vector $\boldsymbol{\varepsilon}$ in Eq. (11) as a spherical unit vector:

$$\boldsymbol{\varepsilon} = -\frac{1}{\sqrt{2}}(\boldsymbol{e}_x + \mathrm{i}\boldsymbol{e}_y). \tag{30}$$

Then the dipole moment $\boldsymbol{p}(t)$ from Eq. (1) is a vector of constant length, which rotates counterclockwise in the xy-plane. The current density follows from Eq. (14):

$$\boldsymbol{i}(\boldsymbol{r},t) = \frac{i_0}{q_1\sqrt{2}}\mathrm{Re}\langle\{\mathrm{i}\boldsymbol{e}_\rho A(q) + \boldsymbol{e}_\phi[B(q) - A(q)]\}\mathrm{e}^{\mathrm{i}\phi}\rangle, \tag{31}$$

where we have set

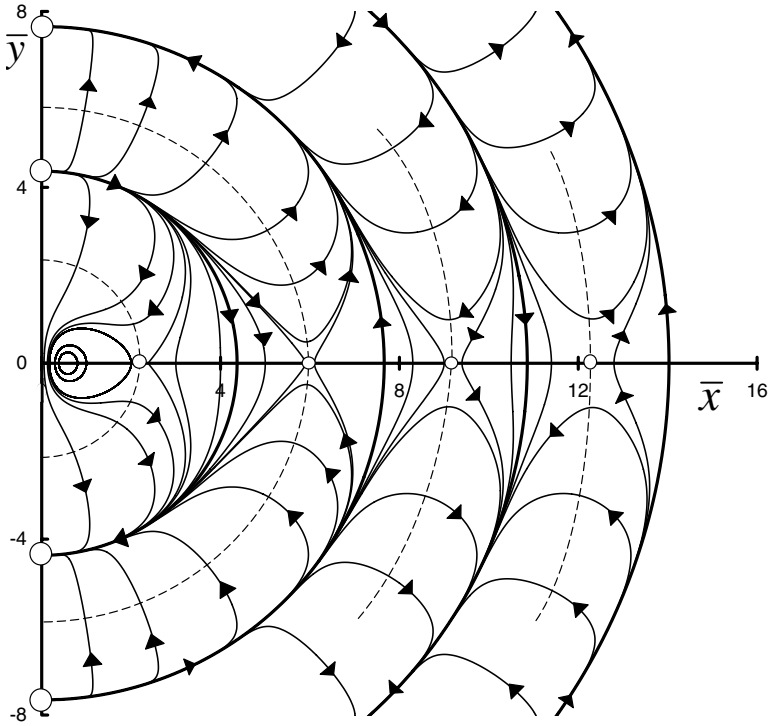

Fig. 6. The figure shows the field line pattern of $\boldsymbol{i}(\boldsymbol{r},t)$ for a magnetic dipole oscillating along the x-axis, for a fixed value of time t, and for $h=1$, $\alpha=0$. The thick and dashed circles are the same as in Fig. 5, but on a different scale. The smallest dashed circle and the corresponding singular point on the $\bar{x}$-axis are not shown. The pattern is symmetric for reflection in the $\bar{y}$-axis.

$$A(q)=\left(1+\frac{i}{q_1}-\frac{1}{q_1^2}\right)\mathrm{e}^{\mathrm{i}(q_1-\alpha)}, \tag{32}$$

$$B(q)=\frac{q^2}{q_1^2}\left(1+\frac{3i}{q_1}-\frac{3}{q_1^2}\right)\mathrm{e}^{\mathrm{i}(q_1-\alpha)}. \tag{33}$$

The $a(q)$ and $b(q)$ from the previous section are the real parts of these $A(q)$ and $B(q)$, respectively. For a point on a field line we use the dimensionless Cartesian coordinates $(\bar{x},\bar{y})$, which are functions of u. From Eq. (31) we then derive the equations for the field lines

$$\frac{\mathrm{d}\bar{x}}{\mathrm{d}u}=\mathrm{Re}\left[\mathrm{i}A(q)-B(q)\frac{\bar{y}}{q^2}(\bar{x}+\mathrm{i}\bar{y})\right], \tag{34}$$

$$\frac{\mathrm{d}\bar{y}}{\mathrm{d}u}=\mathrm{Re}\left[-A(q)+B(q)\frac{\bar{x}}{q^2}(\bar{x}+\mathrm{i}\bar{y})\right], \tag{35}$$

which have to be solved given an initial point $(\bar{x}_0,\bar{y}_0)$.

Each initial point $(\bar{x}_0,\bar{y}_0)$ determines a field line. When we take a large number of initial points, compute the field lines that go through these points, and then draw them all in one figure, we obtain the field line pattern shown in Fig. 7. If we now look at the point indicated by ● in the second quadrant, it seems that one field line comes in and three go out, which would be characteristic of a singular point. However, $\boldsymbol{i}(\boldsymbol{r},t)$ form Eq. (31) has no singular points. In Fig. 8 we show the field line which goes through the initial point (3,2), indicated by ●. We see that the field line spirals in, and when it gets close to the initial point, it turns around, after which it spirals back out. The outgoing spiral lies in between the ingoing spiral. Each field line in Fig. 7 has a similar appearance as the field line in Fig. 8.

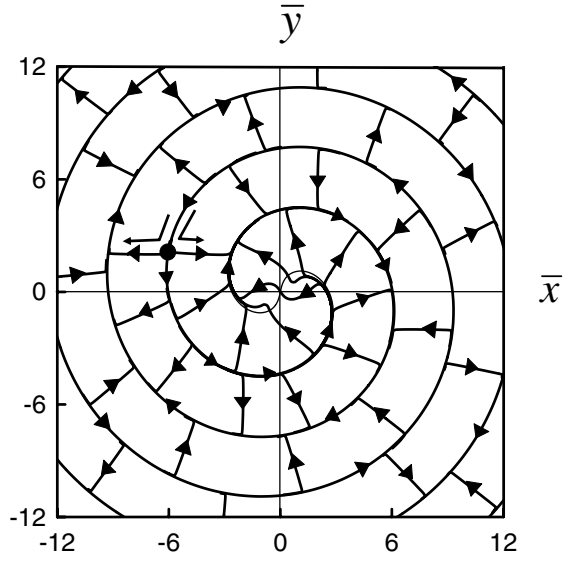

Fig. 7. This figure illustrates the field line pattern of the current density in the surface of the conductor induced by a counterclockwise rotating magnetic dipole on the z-axis, for $h=1$, $\alpha=0$. The spiral of Fig. 9 is copied into this figure as the thin curve, and we notice that it is only visible near the origin. All field lines approximately come in over this spiral and leave following this spiral, so away from the origin, this spiral is covered with field lines. The point indicated as ● in the second quadrant has the appearance of a singular point, but it is not.

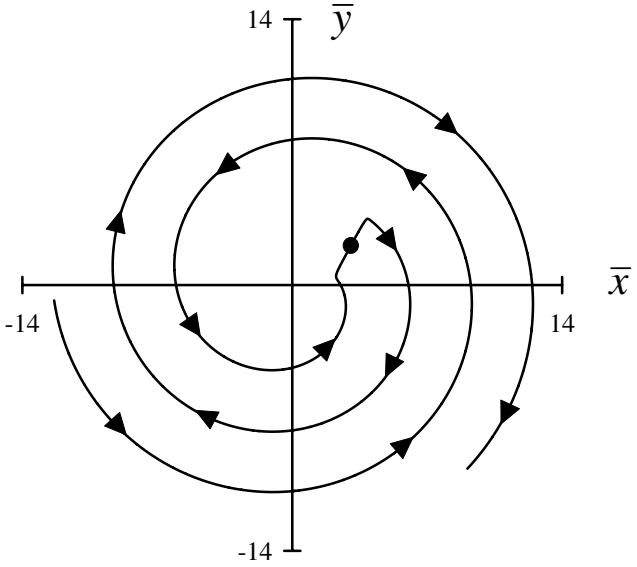

Fig. 8. This figure shows a field line of $\boldsymbol{i}(\boldsymbol{r},t)$ for the case of a rotating dipole moment. The point ● is the initial point, which is (3,2), and the parameters are $\alpha=0$ and $h=1$.

In order to understand the spiraling of the field line, as shown in Fig. 8, we work out expression Eq. (31) more explicitly. This yields

$$\boldsymbol{i}(\boldsymbol{r},t)=-\frac{i_0}{q_1\sqrt{2}}\sqrt{1+\frac{1}{q_1^2}}\left[\boldsymbol{e}_\rho-\frac{1}{q_1}\left(1-\frac{3q^2}{q_1^2}\right)\boldsymbol{e}_\phi\right]\sin(q_1+\delta+\phi-\alpha)+\frac{i_0}{q_1^3\sqrt{2}}[\boldsymbol{e}_\rho\sin(q_1+\phi-\alpha)-h^2\boldsymbol{e}_\phi\cos(q_1+\phi-\alpha)], \quad (36)$$

where we have set

$$\delta=\arctan(1/q_1). \quad (37)$$

We now consider the current density at field points not too close to the origin, so that we can consider q as relatively large. When we neglect terms that drop off faster than $1/q$, Eq. (36) simplifies to

$$\boldsymbol{i}(\boldsymbol{r},t)\approx-\frac{i_0}{q_1\sqrt{2}}\boldsymbol{e}_\rho\sin(q_1+\delta+\phi-\alpha). \quad (38)$$

Since $\boldsymbol{i}(\boldsymbol{r},t)$ is (approximately) proportional to $\boldsymbol{e}_\rho$, it is in the radial direction, either inward or outward depending on the sign of $\sin(q_1+\delta+\phi-\alpha)$. But $\sin(q_1+\delta+\phi-\alpha)$ is a function of the coordinates (q,ϕ), so if we follow a field line in the radial direction we will eventually approach a point where $\sin(q_1+\delta+\phi-\alpha)$ is equal to zero. If we would pass such a point by going in the radial direction, the current density would abruptly go from radially outward to radially inward, or vice versa, which would only be allowed when such a point would be a singular point, which it is not. When we approach a point where $\sin(q_1+\delta+\phi-\alpha)$ is equal to zero, the approximation of Eq. (38) is not valid anymore. The right-hand side goes to zero, and therefore it is not the leading term anymore for the general expression given by Eq. (36). When $\sin(q_1+\delta+\phi-\alpha)=0$, the first term of the right-hand side of Eq. (36) vanishes, and the leading term now becomes

$$\boldsymbol{i}(\boldsymbol{r},t)\approx-\frac{i_0h^2}{q_1^3\sqrt{2}}\boldsymbol{e}_\phi\cos(q_1+\phi-\alpha). \quad (39)$$

Here we have also used that $\delta\to0$ for q sufficiently large, so that $\sin(q_1+\phi-\alpha)\approx0$. We then also have $\cos(q_1+\phi-\alpha)\approx\pm1$. Now we see from Eq. (39) that when a field point is in the neighborhood of a point where $\sin(q_1+\delta+\phi-\alpha)$ is equal to zero, the current density is in the $\boldsymbol{e}_\phi$ direction, either clockwise or counterclockwise. The field line now becomes spiraling with the origin as center, as in Fig. 8. Let us now consider the solution of

$$\sin(q_1+\delta+\phi-\alpha)=0. \quad (40)$$

This equation determines curves in the xy-plane, and when we see q as the variable, the solution for $\phi(q)$ is

$$\phi(q)=-q_1-\delta+\alpha+n\pi,\quad 0\leqslant q<\infty. \quad (41)$$

Here, the right-hand side is a function of q, with α and h fixed parameters, and n is an integer. The corresponding dimensionless Cartesian coordinates for points on the curves are

$$\bar{x}=q\cos\phi(q), \quad (42)$$

$$\bar{y}=q\sin\phi(q). \quad (43)$$

Each value of n then determines a curve, but we only need to consider $n=0$ and $n=1$, since any other value of n reproduces one of these two curves. From Eqs. (42) and (43) we notice that for $q=0$ we have $\bar{x}=\bar{y}=0$, and therefore both curves connect at the origin. When we differentiate Eq. (41) with respect to q, using Eqs. (6) and (37), we obtain

$$\frac{\mathrm{d}\phi}{\mathrm{d}q}=-\frac{qq_1}{1+q_1^2}, \quad (44)$$

which is negative. Therefore, ϕ decreases with increasing q, which gives the curves a spiraling behavior. For q sufficiently large we have $\mathrm{d}\phi/\mathrm{d}q\approx-1$, and therefore q increases by about 2π when ϕ decreases by 2π, e.g., after one rotation of the spiral. For $\phi(q)$ given by Eq. (41) we have $\cos(q_1+\phi-\alpha)\approx\cos(n\pi)$, when we consider $\delta\approx0$. Consequently, $\cos(q_1+\phi-\alpha)\approx1$ for the $n=0$ curve, and from Eq. (39) we then observe that $\boldsymbol{i}(\boldsymbol{r},t)$ near this curve is in the negative $\boldsymbol{e}_\phi$ direction, so the field line rotates clockwise. Similarly, near the $n=1$ curve the current density is in the counterclockwise direction. We now assign the same orientations to the two curves. The $n=0$ curve is defined to run clockwise and the $n=1$ curve goes counterclockwise. On the counterclockwise curve, ϕ increases along the curve and therefore q decreases, so this curve spirals inward from infinity to the origin. In the same way, the $n=0$ curve spirals outward from the origin. This outgoing curve

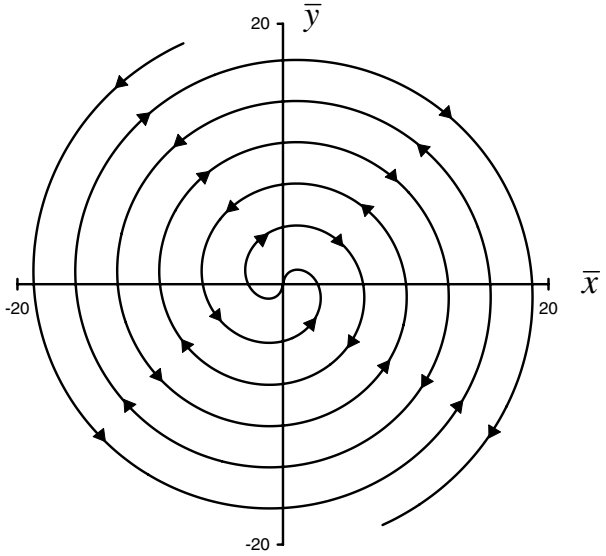

Fig. 9. This figure shows the spiral defined by Eq. (41) with $n = 0$ and $n = 1$, for $h = 1$, $\alpha = 0$. The direction is chosen such that the field lines of the current density follow this spiral, both coming in and going out. The $n = 1$ branch is the incoming part, which rotates counterclockwise and the $n = 0$ branch is the outgoing part which rotates clockwise. Both branches connect smoothly at the origin, where the incoming spiral goes over in the outgoing spiral. The field lines of the current density shown in Fig. 7 come in over this spiral, turn around somewhere near a chosen point, and they leave again over the outgoing branch of this spiral.

spirals outward in between the incoming spiral. This is illustrated in Fig. 9.

When we select an initial point $(\bar{x}_0, \bar{y}_0)$, like the point ● in Fig. 8, the field line through this point will typically run in the radial direction, according to Eq. (38). When we follow the field line over a distance of at most π, it will approach a point on the spiral, and there it will turn in the $\boldsymbol{e}_\phi$ direction. Then it will follow the spiral from there on. When we look at the initial point ● in Fig. 8 we see that the field line comes in over the counterclockwise spiral, until it gets close to chosen point $(\bar{x}_0, \bar{y}_0)$, where it turns into the radial direction. After passing through the initial point, it meets up with the spiral again, after which the field line runs outward over the clockwise part of the spiral. Therefore, all field lines come in over the same spiral, go through a chosen point, and leave again following the clockwise part of this spiral. This gives the field line picture of Fig. 7 for a rotating dipole moment above the xy-plane.

7. Poynting vector at the surface

Fig. 1 shows two field lines of the Poynting vector for an $m = 1$ dipole in free space. An $m = 1$ dipole has a rotating dipole moment, as considered in the previous section. When this dipole is located on the z-axis, a distance H above the conducting xy-plane, it induces the current density pattern shown in Fig. 7. We now consider the Poynting vector and its field lines near the surface, so just above the induced current. The Poynting vector for time-harmonic fields, indicating the direction of energy flow, is in general

$$\boldsymbol{S}(\boldsymbol{r}) = \frac{1}{2\mu_0}\mathrm{Re}\boldsymbol{E}(\boldsymbol{r}) \times \boldsymbol{B}(\boldsymbol{r})^*. \tag{45}$$

Here, oscillations with twice the optical frequency have been dropped, since they average out to zero on a time scale of an optical cycle. This makes $\boldsymbol{S}(\boldsymbol{r})$ independent of time. The complex amplitude of the electric field near the surface can be found by considering the field of the dipole and its mirror image, just as in Section 3, with result

$$\boldsymbol{E}(\boldsymbol{r}) = \frac{k_0^3}{2\pi\varepsilon_0 c}\frac{q}{q_1}\boldsymbol{p}_\parallel \times \boldsymbol{e}_\rho\left(1 + \frac{i}{q_1}\right)\frac{\mathrm{e}^{\mathrm{i}q_1}}{q_1}. \tag{46}$$

The field is perpendicular to the surface, as required by the boundary conditions near a perfect conductor. With $\boldsymbol{B}(\boldsymbol{r})$ given by Eq. (9) we obtain for the Poynting vector

$$\boldsymbol{S}(\boldsymbol{r}) = \frac{i_0^2}{2\varepsilon_0 c}\frac{q}{q_1^3}\mathrm{Re}\left\{(\boldsymbol{\varepsilon}_\parallel \cdot \boldsymbol{e}_\phi)\left[\left(1 - \frac{i}{q_1^3}\right)\boldsymbol{\varepsilon}_\parallel^* \times \boldsymbol{e}_z + \frac{q}{q_1^2}\left(1 - \frac{2i}{q_1} - \frac{3i}{q_1^3}\right)\left(q\boldsymbol{\varepsilon}_\parallel^* \cdot \boldsymbol{e}_\rho - h\varepsilon_\perp^*\right)\boldsymbol{e}_\phi\right]\right\}, \tag{47}$$

where we have used Eq. (11) for $\boldsymbol{p}$. Vector $\boldsymbol{S}(\boldsymbol{r})$ is in the xy-plane for all $\boldsymbol{r}$, indicating that no energy flows into the material.

In Eq. (46) the dipole moment only enters as $\boldsymbol{p}_\parallel$. If the dipole moment is oriented along the z-axis, as considered in Section 4, we have $\boldsymbol{p}_\parallel = 0$, and therefore $\boldsymbol{E}(\boldsymbol{r}) = 0$ in the xy-plane, which then gives $\boldsymbol{S}(\boldsymbol{r}) = 0$. Apparently, for the current density field line pattern shown in Fig. 3, the corresponding Poynting vector is zero. The complex amplitude $\sigma(\boldsymbol{r})$ of the surface charge density follows from the electric field near the surface according to

$$\sigma(\boldsymbol{r}) = \varepsilon_0 \boldsymbol{e}_z \cdot \boldsymbol{E}(\boldsymbol{r}), \tag{48}$$

just like $\boldsymbol{i}(\boldsymbol{r})$ followed from $\boldsymbol{B}(\boldsymbol{r})$ with Eq. (5). This implies that for the case of a dipole moment along the z-axis the induced surface charge density is zero. From conservation of charge we have $\nabla \cdot \boldsymbol{i}(\boldsymbol{r}) = \mathrm{i}\omega\sigma(\boldsymbol{r})$, and it should therefore hold that the field line pattern in Fig. 3 has a zero divergence. That this is indeed the case can be seen from Eq. (15). The current density only has an $\boldsymbol{e}_\phi$ component, and this component is independent of ϕ. Any such vector field in a plane has a zero divergence.

8. Dipole moment along the x-axis

We now consider a dipole moment $\boldsymbol{p}$ along the x-axis, as in Section 5. When we set $\boldsymbol{\varepsilon}_\parallel = \boldsymbol{e}_x$, $\varepsilon_\perp = 0$ in Eq. (47) and express the result in Cartesian coordinates we obtain

$$\boldsymbol{S}(\boldsymbol{r}) = \frac{i_0^2}{2\varepsilon_0 c}\frac{\bar{y}}{q_1^5}[\bar{x}\bar{y}\boldsymbol{e}_x + (\bar{y}^2 + h^2)\boldsymbol{e}_y]. \tag{49}$$

We first notice that $\boldsymbol{S}(\boldsymbol{r}) = 0$ for $\bar{y} = 0$, and therefore the $\bar{x}$-axis is a singular line. Second, when we replace $\bar{x}$ by $-\bar{x}$ and leaving $\bar{y}$ the same, then the $\bar{x}$-component of

$\boldsymbol{S}(\boldsymbol{r})$ changes sign, whereas the $\bar{y}$-component remains the same. Therefore the field line pattern of $\boldsymbol{S}(\boldsymbol{r})$ is symmetric under reflection in the $\bar{y}$-axis, so here we only consider $\bar{x} \geqslant 0$. Third, when we set $\bar{x} = 0$ we get $\boldsymbol{S}(\boldsymbol{r}) \propto \bar{y}\boldsymbol{e}_y$, so for a point on the $\bar{y}$-axis the Poynting vector is along the $\bar{y}$-axis, and such that it is directed up for $\bar{y} > 0$ and down for $\bar{y} < 0$. Therefore the positive and negative parts of the $\bar{y}$-axis are field lines, and $\bar{y} = 0$ is a singular point dividing the two parts.

The field lines of $\boldsymbol{S}(\boldsymbol{r})$ follow from Eq. (27) with $\boldsymbol{i}$ replaced by $\boldsymbol{S}$. In a similar way as in Section 5 we then find the equations for the field lines

$$\frac{\mathrm{d}\bar{x}}{\mathrm{d}u} = \bar{x}\bar{y}^2, \tag{50}$$

$$\frac{\mathrm{d}\bar{y}}{\mathrm{d}u} = \bar{y}(\bar{y}^2 + h^2), \tag{51}$$

from which

$$\frac{\mathrm{d}\bar{x}}{\mathrm{d}\bar{y}} = \frac{\bar{x}\bar{y}}{\bar{y}^2 + h^2}. \tag{52}$$

This equation is separable, and the field line that goes through the point $(\bar{x}_0, \bar{y}_0)$ is found to be

$$\bar{x} = \bar{x}_0 \sqrt{\frac{\bar{y}^2 + h^2}{\bar{y}_0^2 + h^2}}. \tag{53}$$

Here we see $\bar{y}$ as the independent variable, which can be positive or negative. Replacing $\bar{y}$ by $-\bar{y}$ has no effect, so the field line pattern is symmetric for reflection in the $\bar{x}$-axis. Fig. 10 shows the field line picture. All field lines start on the $\bar{x}$-axis, which is a singular line, and run to infinity. Let us take $\bar{y}_0 = 0$, so that $\bar{x}_0$ is the $\bar{x}$-coordinate of the initial point which is now on the $\bar{x}$-axis. Then for $\bar{y}$ large, the field lines approach the asymptotic line $\bar{y} = (h/\bar{x}_0)\bar{x}$ for $\bar{y} > 0$, which is a line through the origin with slope $h/\bar{x}_0$. This slope gets smaller with increasing $\bar{x}_0$, as can also be seen from the figure.

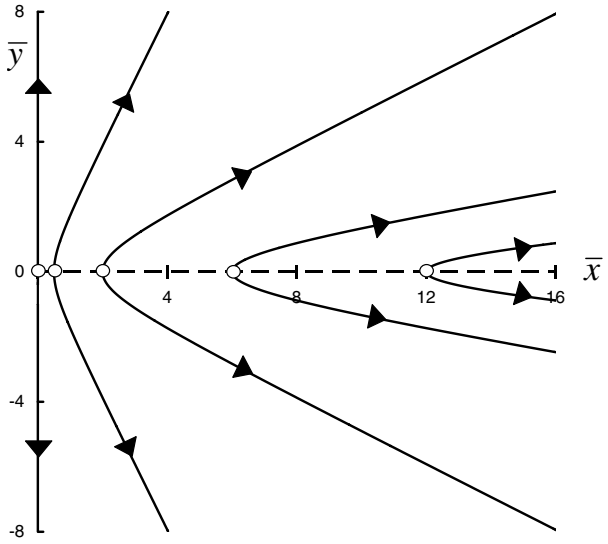

Fig. 10. The figure shows the field lines for the Poynting vector in the $\bar{x}\bar{y}$-plane for the case of a dipole moment along the x-axis, and with $h = 1$. The field lines start on the $\bar{x}$-axis, which is a singular line, and then run to infinity where they approach asymptotically a straight line through the origin.

9. Dipole moment rotating in the xy-plane

Finally we consider a dipole moment that rotates in the xy-plane, as in Section 6. With $\boldsymbol{\varepsilon}$ given by Eq. (30), the Poynting vector becomes

$$\boldsymbol{S}(\boldsymbol{r}) = \frac{i_0^2}{4\varepsilon_0 c}\frac{q}{q_1^3}\left\{\boldsymbol{e}_\rho + \frac{1}{q_1^3}\left[q^2\left(2 + \frac{3}{q_1^2}\right) - 1\right]\boldsymbol{e}_\phi\right\}. \tag{54}$$

We see that the origin of coordinates is a singular point, due to the overall factor of q, and that for q large the field lines run approximately in the outward radial direction. For the equations for the field lines we now use polar coordinates (q,ϕ) in the $\bar{x}\bar{y}$-plane. We then obtain

$$\frac{\mathrm{d}q}{\mathrm{d}u} = 1, \tag{55}$$

$$q\frac{\mathrm{d}\phi}{\mathrm{d}u} = \frac{1}{q_1^3}\left[q^2\left(2 + \frac{3}{q_1^2}\right) - 1\right]. \tag{56}$$

This set can be solved by elementary methods, and the result is

$$\phi(q) = \phi_0 - \frac{1}{2h^3}\ln\left(\frac{q_1 - h}{q_1 + h}\right) - \frac{1}{q_1}\left(2 + \frac{1}{h^2} + \frac{1}{q_1^2}\right), \quad 0 < q < \infty. \tag{57}$$

Here we see q as the independent parameter. The Cartesian coordinates for points on a field line are given by Eqs. (42) and (43), which show that the field lines start at the origin of coordinates. In Eq. (57) ϕ_0 is an arbitrary constant, which is equal to $\phi_0 = \phi(\infty)$, and each choice of ϕ_0 determines a field line. For a given h, the different field lines only differ in their values of ϕ_0, and therefore they all have the same shape. Changing ϕ_0 simply rotates the curve in the $\bar{x}\bar{y}$-plane.

Fig. 11 shows a field line for $\phi_0 = 0$. For $q = 0$ we have $q_1 = h$, and the logarithm in Eq. (57) is $-\infty$. Therefore we have $\phi(0) = \infty$. When q increases, $\phi(q)$ becomes finite, so it decreases, which gives a clockwise rotation of the field line around the origin. We conclude that the Poynting vector has a vortex at the origin of coordinates. On the other hand, for q large we find from Eq. (57) by Taylor expansion

$$\phi(q) \approx \phi_0 - \frac{2}{q}. \tag{58}$$

When q increases here, $\phi(q)$ increases, and this gives a counterclockwise rotation, until $\phi(q)$ approaches its asymptotic value of ϕ_0. For q large we have $\phi(q) \approx \phi_0$, and one may expect that the field line approaches a straight line through the origin, making an angle ϕ_0 with the positive $\bar{x}$-axis, which would be the case if we would have $\phi(q) = \phi_0$. However,

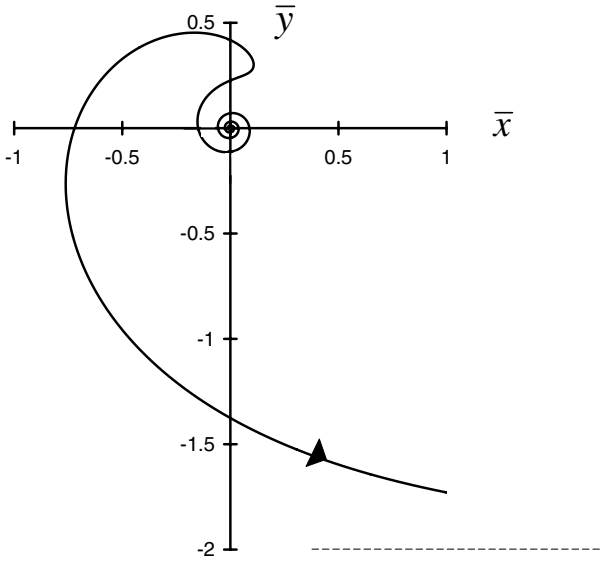

Fig. 11. Shown is a field line of the Poynting vector in the $\bar{x}\bar{y}$-plane for a rotating dipole moment, a distance $H = 0.5/k_0$ above the xy-plane. This field line is represented by Eq. (57) with $\phi_0 = 0$. The field line starts at the origin, spirals out clockwise, then changes to a counterclockwise rotation, and eventually it levels off to the asymptote $\bar{y} = 2$, indicated by the dashed line.

from Eq. (58) we obtain $\cos\phi(q) \approx \cos\phi_0 + (2/q)\sin\phi_0$, and since we have $\bar{x} = q\cos\phi(q)$, the second term gives a finite contribution for q large. The same holds for $\bar{y}$ from Eq. (43), and when we eliminate q as the independent variable we find the equation for the asymptote of the field line to be

$$\bar{y} = \bar{x}\tan\phi_0 - \frac{2}{\cos\phi_0}. \tag{59}$$

This line does not go through the origin, but has a $\bar{y}$ intercept of $-2/\cos\phi_0$. For $\phi_0 = 0$, as in Fig. 11, the asymptote is $\bar{y} = -2$.

10. Conclusions

We have studied the current density on the surface of a perfect conductor, induced by a nearby oscillating magnetic dipole. For a dipole moment along the z-axis, the field lines are clockwise and counterclockwise running circles, separated by singular circles. For a linear dipole moment which is oriented parallel to the surface, we found the complex field line pattern shown in Fig. 6. The field lines are loops which start at a singular point on the y-axis and end on another singular point on the y-axis. Near the origin of coordinates there are also field lines which form closed loops, circling around a singular point on the x-axis. When the dipole moment rotates in the xy-plane, the field line pattern is determined by the spiral of Fig. 9. Field lines run inward along the spiral, turn around near a chosen point, and then run back outward along the spiral. We have also considered the field lines of the Poynting vector near the surface for the same orientations of the dipole. It was found that for a dipole moment along the z-axis the Poynting vector near the surface vanishes as a result of the fact that the induced surface charge density is zero. For a linear dipole moment parallel to the surface the field lines of the Poynting vector are illustrated in Fig. 10, and for a dipole moment rotating parallel to the surface the Poynting vector has a vortex at the origin of coordinates, as shown in Fig. 11.

References

[1] J.F. Nye, M.V. Berry, Proc. R. Soc. Lond. A 336 (1974) 165.
[2] W. Braunbek, G. Laukien, Optik 9 (1952) 174.
[3] H.F. Schouten, T.D. Visser, G. Gbur, D. Lenstra, H. Blok, Opt. Exp. 11 (2003) 371.
[4] H.F. Schouten, T.D. Visser, G. Gbur, D. Lenstra, H. Blok, Phys. Rev. E 67 (2003), 036608-1-3.
[5] M. Vasnetsov, K. Staliunas (Eds.), Optical Vortices, Horizons in World Physics, vol. 228, Nova Science, Commack, New York, 1999.
[6] A.V. Volyar, V.G. Shvedov, T.A. Fadeeva, Opt. Spectrosc. 90 (2001) 93.
[7] V.A. Pas'co, M.S. Soskin, M.V. Vasnetsov, Opt. Commun. 198 (2001) 49.
[8] A.V. Volyar, T.A. Fadeeva, V.G. Shvedov, Opt. Spectrosc. 93 (2002) 285.
[9] S.M. Barnett, L. Allen, Opt. Commun. 110 (1994) 670.
[10] M.S. Soskin, M.V. Vasnetsov, in: E. Wolf (Ed.), Progress in Optics, vol. 42, Elsevier, Amsterdam, 2001, p. 219.
[11] H.F. Arnoldus, Opt. Commun. 252 (2005) 253.
[12] H.F. Arnoldus, J.T. Foley, Opt. Commun. 231 (2004) 115.
[13] J.D. Jackson, Classical Electrodynamics, third ed., Wiley, New York, 1999.
[14] H.F. Arnoldus, Surf. Sci. 590 (2005) 101.